

# Multiple Ionization in Strong Fields

J. Ullrich<sup>1</sup>, R. Dörner<sup>2</sup>, R. Moshhammer<sup>1</sup>, H. Rottke<sup>3</sup>, W. Sandner<sup>3</sup>

<sup>1</sup>*Max-Planck-Institut für Kernphysik, Saupfercheckweg 1, D-69117 Heidelberg*

<sup>2</sup>*Insitut für Kernphysik, August Euler Str. 6, D-60486 Frankfurt*

<sup>3</sup>*Max-Born-Institut, Max-Born-Str. 2a, D-12489 Berlin*

Using “Reaction Microscopes” that enable to detect the vector momenta of several electrons and ions after fragmentation of atoms or molecules, pathways for multiple electron ejection in femtosecond PW/cm<sup>2</sup> Laser fields have been explored in unprecedented detail. Classical boundaries for “recollision”, which is identified to be the dominant multiple ionization mechanism, are analyzed. The electron-electron correlation in Ne double ionization is explored, Coulomb repulsion between the emerging electrons is demonstrated for Ar double ionization, the importance of excitation – field-ionization mechanisms is elucidated and sub-threshold multiple ionization processes are discussed. Future possibilities as the realization of an “attosecond streak-camera” at free electron lasers are envisaged.

## 1 Introduction

The interaction of intense coherent light, as routinely realized nowadays using Ti:Sa lasers (800 nm, 1.5 eV) at typical pulse lengths below 100 fs and intensities of more than 10<sup>16</sup> W/cm<sup>2</sup> (see e.g. [1]) with atoms, molecules, clusters or solids has attracted increasing attention in the recent past. Single electron emission, the intensity dependence of ion rates, multiple ionization yields, dissociation of molecules, harmonic generation etc. have been explored in detail over many years essentially using single particle detection techniques (see e.g. [2]). Thus, a profound theoretical understanding of non-linear multi-photon processes that either involve only one electron or where electrons can be considered to act independently has emerged within a single active electron description (see e.g. [3]).

In contrast, the correlated motion of several electrons and ions, their time-dependent dynamics in the field, pathways to multiple ionization or the dissociation of molecules cannot be treated by ab initio theories even for the most simple reactions like He double ionization. Accordingly, they have remained subject of numerous controversial debates over the last decade (e.g. [4]). Only two years ago, many-particle imaging techniques that monitor the final-state vector momenta of several electrons and ions with high resolution and large acceptance, developed to explore fragmentation of atoms and molecules in collisions with charged particles and single photons [5,6], have been successfully employed for the first time to study few particle correlated dynamics in laser pulses interacting with single atoms or molecules.

The present article tries to summarize the wealth of new results on fragmentation of atoms obtained using these next-generation methods (see also [7]). After a very short description of the imaging technique in section 3, a selection of illustrative experimental results is presented in section 4 with references to available theoretical predictions. Future possibilities are envisaged in section 5.

## 2 “Reaction Microscopes”

Within the last decade, many-particle momentum spectroscopy of ions and electrons has been developed to investigate ionization dynamics in fast heavy-ion – atom collisions. These instruments, so-called Reaction Microscopes, turned out to be extremely versatile and were subsequently used for the investigation of multiple-ionization or molecular break-up dynamics induced by impact single photons, laser-pulses, antiparticles or electrons. Only the salient features of the spectrometer will be summarized here, details can be found in references [8,9].

As illustrated in Figure 1, the laser beam is focused by a spherical on-axis mirror to a typical diameter of  $10\ \mu\text{m}$  onto a low-density ( $10^7\ \text{atom}/\text{cm}^3$ ) supersonic, internally cold ( $T \sim 1\ \text{K}$ ) atomic gas-jet target. Recoiling ions and electrons emitted during the collision are guided by homogeneous electric and magnetic fields to multi-hit, position-sensitive multi-channel plate detectors, mounted perpendicular to the laser beam propagation at a distance of about 20 cm from the reaction volume. From the times-of-flight (coincidence with the Q-switch laser trigger) and the positions of arrival, the initial vector momenta of the fragments are calculated from the equations of motion for electrons and ions in the well-known electric and magnetic fields.

By varying the magnitude of the projection fields, both the resolution as well as the acceptance for the fragments in momentum space that are projected, can be chosen over a wide range. Typically, for one setting, all ions of interest with momenta  $|\mathbf{P}_R| < 5\ \text{a.u.}$  are accepted simultaneously (a.u.: atomic unit). At the same time, all electrons with transverse energies (transverse to the extraction field)  $E_{e\perp} < 50\ \text{eV}$  as well as with longitudinal energies of  $E_{e\parallel} < \infty\ \text{eV}$  into the forward (towards the detector), and  $E_{e\parallel} < 15\ \text{eV}$  into the backward directions are detected. Up to ten hits on the electron detector are accepted for a minimum time between two hits of 15 ns in case that both electrons hit the detector within a distance of less than 1 cm. For all other events electrons can be detected on the 80 mm diameter detector even if they hit the detector at identical times. The position resolution of the delay-line read-out system can be as good as  $100\ \mu\text{m}$ . Depending on the magnitude of electric ( $\sim 1\text{-}2\ \text{V}/\text{cm}$ ) and

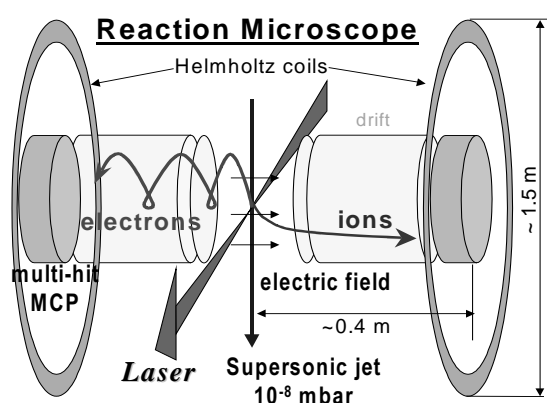


Figure 1: Experimental set-up. Electrons and ions emerging from the fragmentation of a single atom or molecule from a supersonic jet-target are projected by electric and magnetic fields onto position and time-sensitive multi-hit multichannel plate (MCP) detectors. From the list-mode data three dimensional momentum vectors of all particles can be calculated (see text).

magnetic fields (typically 15 G up to 50 G) chosen in the specific experiment the Reaction Microscope is able to simultaneously monitor up to 90 % of the nine-dimensional final-state momentum space for double ionization.

Superior electron momentum resolution of  $\Delta |\mathbf{P}_e| = 0.05$  a.u. corresponding to an energy resolution of  $\Delta E_e = 34$  meV for electrons close to zero energy in the continuum is achieved. Limited by the internal jet temperature typical ion momentum resolutions are 0.1 a.u. transverse and 0.2 a.u. along the jet propagation, corresponding to energy resolutions of 19  $\mu\text{eV}$  or 74  $\mu\text{eV}$  for low-energy ions, respectively.

Experiments with intense lasers are exceptionally challenging for the following reasons: First, the rest gas pressure as well as the target density has to be extremely small, since the laser pulse ionizes all particles within its focus of about 10  $\mu\text{m}$  diameter. Thus, as correlated emission of electrons and ions from the same atom shall be measured, only one target atom is allowed to be in the focus of the laser pulse and, accordingly, the target is operated at a very low density at a background pressure of  $2 \cdot 10^{-11}$  Torr. Second, since at maximum only one atom shall be ionized per laser pulse in order to maintain information about the correlation, high repetition rates are mandatory. Whereas charged particle or single photon impact experiments are run with a typical repetition rate of up to 1 MHz, state-of-the-art high-power Ti:Sa lasers operate at repetition rates of typically 1 kHz with an upper limit of 5 kHz for commercial systems. At lower intensities, 100 kHz systems have recently been used at the Max-Planck-Institut for Quantum-Optics in Munich [10].

For those reasons, though typical measuring times are several days, all laser experiments still suffer from limited statistical significance and no kinematically complete measurements have been performed for double and multiple ionization up to now. This situation might change in the near future due to expected rapid progress in the performance of high-power lasers on the one hand, but, even more important, due to the advent of VUV and soft X-ray self-amplified free electron lasers which presently work at a repetition rate of 70 kHz with 1 MHz being envisaged.

## 2 Results

### Non-Sequential and Sequential Ionization: Phase Dependence in the Field

In Figure 2 ion-momentum distributions parallel ( $P_{\parallel}$ ) and perpendicular ( $P_{\perp}$ ) to the laser polarization axis are shown for  $\text{Ne}^{1+}$  and  $\text{Ne}^{2+}$  created in intense, linear polarized laser fields in the sequential and non-sequential regime at a pulse length of 25 fs. The experiments were performed at the Max-Born-Institute in Berlin. Similar data have been published for He [11] and Ar [12,13]. Striking differences are observed between single (1) and double ionization (2) in an intensity regime where double ionization is dominated by non-sequential (NS) mechanisms [14]. Whereas the comparably narrow distribution without any ATI structure (above threshold ionization) for singly charged ions is well described by tunneling ionization (at a Keldish parameter [15] of  $\gamma = 0.35$ ), a pronounced double peak structure along the polarization direction was found for double and triple ionization [16]. This structure automatically rules out “shake-off” [17] or “collective tunneling” [18] as dominant NS double ionization mechanism as will be illustrated below. On the other hand, the peaks were

found to be compatible with the “antenna -” [20] or the “recollision mechanism” [21] as was first shown within classical considerations [16,19]. Subsequently, a variety of theoretical predictions (see the detailed discussion and references in [7]) based on S-matrix theory, on the numerical solution of the time dependent Schrödinger equation (TDSE) as well as on the classical or semi-classical approximations essentially established the double peak-structure and recollision as the dominant NS double ionization mechanism. Experimentally, this was even evident before from measurements with circularly polarized light [22,23]. In the sequential regime a broader distribution is observed with a single peak at zero momentum along the field axis (3).

Interestingly, the ability of the experiments to distinguish between different dynamic ionization mechanisms relies on the simple nevertheless remarkable fact that the ion momenta can, under certain conditions, provide information on the phase  $\varphi = \omega t_1$  ( $\omega$ : laser frequency) of the time-dependent laser field  $\mathbf{E}(t) = \mathbf{E}_0 \cdot \sin(\omega t)$  where (multiple) ionization took place, i.e. at what phase the ion was born. This is immediately obvious from a classical treatment [16,19] but is also inherent to the all quantum calculations mentioned above. If an ion is created with charge  $q$  and zero initial momentum at a time  $t_1$  in a pulse that is long compared to the oscillation period ( $\tau\omega \gg 1$ ,  $\tau$ : pulse duration), the final ionic drift momentum parallel to the laser field only depends on the phase  $P(t_1) = (q/\omega) \cdot E_0 \cdot \cos(\omega t_1)$  with a maximum momentum of  $P^{\max}(t_1) = 2q(U_p)^{1/2}$  ( $U_p = E_0^2/4\omega^2$ : ponderomotive potential). At a laser frequency of  $\omega = 0.05$  a.u. and a field amplitude  $\mathbf{E}(t) = 0.18$  a.u. ( $10^{15}$  W/cm<sup>2</sup>) a typical momentum resolution for singly charged ions of 0.1 a.u. would, thus, directly translate in a phase resolution of up 3 % of a full optical cycle i.e. to a time resolution 80 as.

The exact “tracing” of the phase by measuring the ion drift momentum is disturbed by any momentum transferred to the ion when it is created by a certain process like “tunneling”, multi-photon absorption or “rescattering”. This leads to a reduced, however, often still sufficient phase resolution, as is impressively demonstrated for NS double ionization: “Rescattering”, where double ionization is due to an ionizing collision between the first electron being accelerated in the laser field and thrown back on its parent ion, mainly occurs at a phase where the electric field is

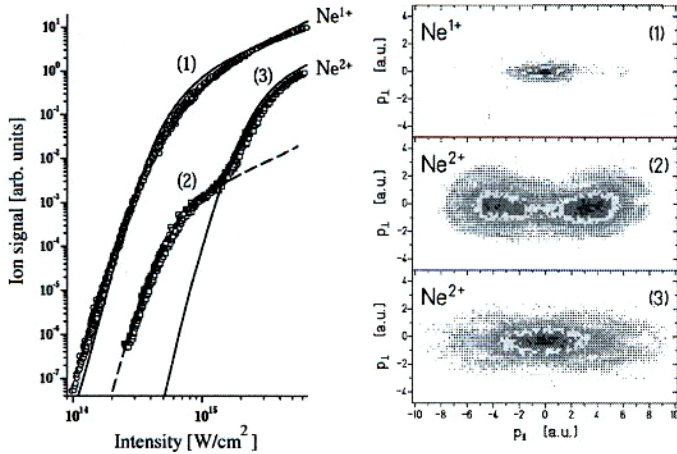


Figure 2: Ne double ionization by 800 nm, 25 fs laser pulses. Left:  $\text{Ne}^{1+}$ ,  $\text{Ne}^{2+}$  yields as a function of the laser intensity (from [14]). Solid lines: Independent event model. Right hand side: ion momentum distributions for different intensities (see text).

close to zero i.e. at  $\omega \cdot t_1 = n \cdot \pi$  (with  $n = 1, 2, \dots$ ) resulting in a large drift momentum of the doubly charged ion [16,19]. In contrast, zero average drift momentum is expected for the other two NS double ionization mechanisms that have been proposed, “shake-off” and “collective tunneling”, since for both double ionization is most likely to occur at maximum field strength, i.e. for a phase  $\omega \cdot t_1 = (2n + 1) \cdot \pi/2$  (with  $n = 0, 1, 2, \dots$ ). The various mechanisms can only be distinguished in an unambiguous way by an ion momentum measurement alone, however, if the momentum transfer during creation of the ion by the one or other mechanism is less than the difference in drift momenta of the ions resulting from the average phase difference where the processes occur. In this case well separated maxima are visible in the ion momentum distributions along the electric field direction.

### Correlated Motion of Electrons in the Sequential and Non-Sequential Regimes

Having provided evidence that recollision is the dominant NS double ionization mechanism we now explore the correlated motion of the emitted electrons. In Figure 3 we have plotted the correlated momenta of both electrons along the field direction ( $P_{e\parallel}$ ) for double ionization at  $1 \text{ PW/cm}^2$  for Ar in the sequential (left) and for Ne in the non-sequential (right) regime, respectively. Whereas the electrons behave independently to a large extent for sequential ionization a strongly correlated motion is visible in the NS regime. Here, both electrons are nearly exclusively emitted into the same hemisphere with very similar momenta.

First one might analyze whether the observed distribution is compatible with the recollision model (see also [24]). For a certain tunneling phase of the first electron  $\omega t_0$ , recollision happens at a well defined recollision energy  $E^{\text{recoil}}$  and phase  $\omega t_1$ , the latter resulting in well defined and equal drift momenta of both electrons  $P_{e\parallel}^{\text{drift}}(\omega t_1)$  after the collision. In addition, they can share the excess energy  $E^{\text{ex}} = E^{\text{recoil}} - I_P$  ( $I_P$ : ionization potential). Neglecting the transverse energies of the electrons, energy conservation  $P_{e1\parallel}^2 + P_{e2\parallel}^2 = 2E^{\text{ex}}$  yields a circle with radius  $\sqrt{2E^{\text{ex}}}$  around the points  $(\pm P_{e1}^{\text{drift}}(\omega t_1), \pm P_{e2}^{\text{drift}}(\omega t_1))$  as maximum possible drift momentum combination.

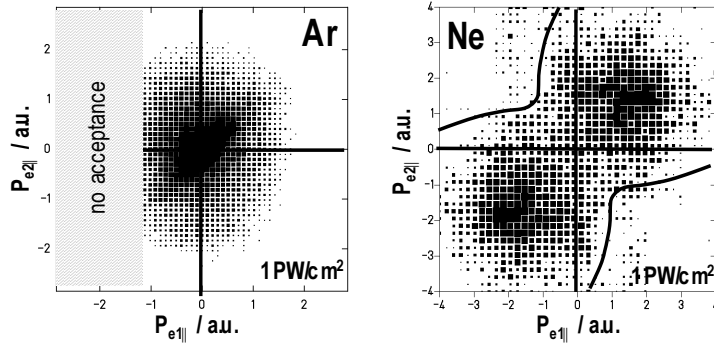


Figure 3: Correlated electron momenta along e polarization axis for double ionization of Ar (left) and Ne (right) at  $1 \text{ PW/cm}^2$ . Full lines: Kinematical boundaries for classical rescattering due to energy and momentum conservation.

Considering all phases the full curved lines for Ne are obtained indicating the classical boundary following from momentum and energy conservation during rescattering inside which all correlated events must occur. The comparison with the experimental data impressively shows that nearly all events are within these boundaries.

A different behavior has been found for Argon [24,25] where the classically allowed regime at an intensity of  $2.5 \cdot 10^{14}$  W/cm<sup>2</sup> is completely restricted to the quadrants with equal emission direction of both electrons, i.e. equal signs of both momenta (Figure 4, left). A large yield of electrons being emitted into opposite hemispheres has been interpreted as excitation during recollision of the still bound electron which then might be field-ionized in one of the subsequent maxima of the oscillating field [24]. In contrast to Ne, the 3p to 3d excitation cross sections are large making such a scenario quite likely. Observed momenta are within the classical kinematical limits for this process which tends to “fill the valley” in-between the two “recollision maxima” in the ion-momentum distribution (projection along the positive diagonal, see the detailed discussion in [24]).

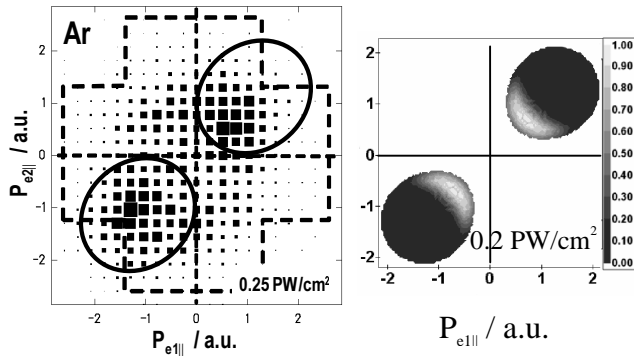


Figure 4: Correlated electron momenta for Ar<sup>2+</sup> creation at 0.25 (left, exp.) and 0.2 PW/cm<sup>2</sup> (right, theory from [26]). Full line: Classical boundaries for recollision. Dotted line: Kinematical limit for excitation during recollision followed by field ionization.

While practically all events are compatible with the kinematical boundaries for recollision in the Ne case the correlation pattern itself, however, with many electrons of quite similar longitudinal momenta is in contradiction with the predictions based on field-free electron-impact (e,2e) ionization dynamics [26] (Figure 4, right), which becomes actually more obvious at higher intensities in [26]. In accordance with the fact that unequal energy sharing between projectile and ionized electron is by far the most likely configuration in (e,2e) at not too low impact energy, unequal final momenta are predicted as well in the NS double ionization in laser fields in striking contrast to the experimental results. Several other predictions, using a hard core form factor for the electron collision or solving the one-dimensional TDSE with correlated electrons are in poor agreement with the experiment. Only recently semi-classical predictions [27] were able to predict a similar pattern as observed in the experiments.

In summary, even if it seems to be out of any question that rescattering is the dominant NS double ionization mechanism, the correlated motion of both electrons in the field is far from being consistently understood theoretically.

### Evidence for Coulomb Repulsion of the Electrons in the Final State

Preferred emission of two electrons with nearly identical momenta along the field direction as observed in the experiment seems to contradict electron-repulsion in the final state. Quantum mechanical calculations solving the one-dimensional TDSE on a grid with fully correlated electrons in the helium atom (Figure 5 left, [28]) observe a minimum for equal  $P_{e\parallel}$ . Here, however, the Coulomb repulsion is certainly overestimated due to the one-dimensionality of the model. Experimentally, we can artificially reduce the dimensions in the final state by the requirement, that the final transverse momentum of one of the electrons - and thus, in a (e,2e) scenario also of the second one - is small. Then, as illustrated in Figure 5b [29,30], the maximum along the diagonal with equal  $P_{e\parallel}$  is significantly depleted. Since now the electrons are restricted in their transverse motion they repel each other more strongly longitudinally.

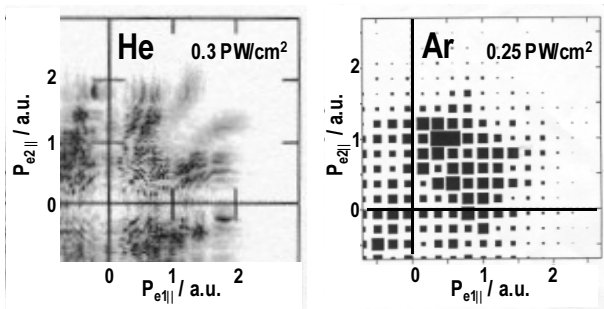


Figure 5: Correlated momenta of electrons for  $\text{He}^{2+}$  (left, theory [28]) and  $\text{Ar}^{2+}$  (right, experiment [29]) creation at indicated laser intensities. Experiment: transverse momentum of electron 1 is smaller than 0.5 a.u.

### Sub-Threshold Recollision at Low Intensity

Very recently, Eremina and co-workers [10] have performed a set of experiments measuring the recoil-ion momentum distributions for  $\text{Ar}^{2+}$  and  $\text{Ne}^{2+}$  ions at low intensities leading to a maximum recollision energies of  $E^{\text{recoil}} = 3.17 \cdot U_p$  well below the ionization potential  $I_p$  of ground-state  $\text{Ar}^+$  or  $\text{Ne}^+$  ions in a field-free environment. Laser pulses of 30 fs (800 nm) were used at the Max-Planck-Institute for Quantum-Optics in Garching at a repetition rate of 100 kHz and 6  $\mu\text{J}$  pulse energy.

In Figure 6, momentum distributions for  $\text{Ar}^{2+}$  and  $\text{Ne}^{2+}$  are shown for various ratios of recollision energies to ionization potentials  $E^{\text{recoil}}/I_p$  ranging from values larger than one, where recollision impact ionization is possible to  $E^{\text{recoil}}/I_p$  as low as 0.5, where the energy of the recolliding electron is well below threshold. The smooth transition between both regimes observed in the ion rates has always been an argument against a simple recollision scenario to explain NS double ionization. The observed momentum distributions for Ar, Ne and He at equal  $E^{\text{recoil}}/I_p$  strongly differ from each other indicating that different mechanisms seem to be active below threshold for the various species. Whereas the valley between the maxima is more and more filled for Ar finally displaying a clear maximum at zero drift momentum for  $E^{\text{recoil}}/I_p = 0.5$ , a clear double peak structure remains for Ne at  $E^{\text{recoil}}/I_p = 0.7$ .

While for argon the transition can be consistently explained by the increased importance of excitation during recollision followed by field ionization in the subse-

quent rise of the oscillating field along the lines discussed above, smoothly “filling the valley”, the pronounced sub-threshold double-hump structure for neon double ionization was explained as increased importance of recollision at a different phase of the field, where it is not zero. Here, the effective ionization potential of  $\text{Ne}^{2+}$  is lowered to such an extent that the re-colliding electron can still ionize the  $\text{Ne}^+$  ion assisted by the field. Thus, more and more but smoothly, different but well-defined and narrow recollision phase intervals become important leading to well defined but lower recoil-ion-momenta and, thus, to a pronounced double-peak structure.

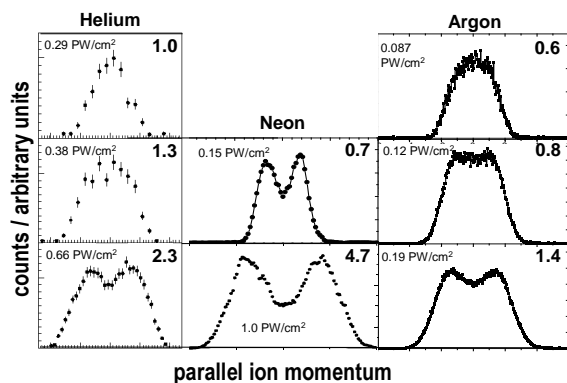


Figure 6: Ion Momentum distributions along the laser polarization direction for He [11], Ne (partly from [16]) and Ar [10]. Respective intensities are indicated in each panel. Upper right number in the panels: Ratio of recollision energy to the ionization potential of the singly charged ion without field.

Surprisingly, the behavior of He (left row in the figure) is strongly different and not consistently to be interpreted within the above argumentation. Therefore, more experimental results for helium, which is the only system where fully quantum-mechanical calculations might be expected within the near future [31] are urgently needed. Such experiments, which are extraordinary challenging since they require a background vacuum of  $10^{-13}$  Torr, comparably high laser intensities at simultaneously high repetition rate are under preparation in several laboratories.

## 4 A View into the Future: An Attosecond Streak Camera

A whole bunch of future investigations might be envisaged: Among them are kinematically complete measurements on molecules (a first one has been reported recently [32]), on state-prepared molecular ions or experiments with very good statistical significance allowing to project fully differential cross sections as routinely done for photon, electron or ion impact. Furthermore, investigations using extreme short laser pulses of only one optical cycle with fixed phase within the envelope, recently demonstrated [33], will certainly be performed. Moreover, pulses will actively be shaped in the future in order to control the electron dynamics such that certain reactions in atoms, molecules or clusters will be either enhanced or suppressed.

A major step forward will be the advent of tunable high-intensity short-pulse VUV or even x-ray self-amplifying (SASE) free-electron lasers (FEL), which have been demonstrated to be realizable in November 2001 [34] in Hamburg. At the TESLA-Test Facility the user operation will start in 2004 with 150 fs,  $10^{17}$  W/cm<sup>2</sup>



pulses at photon energies between 20 and 200 eV, a bandwidth of  $10^{-4}$ , 70 kHz repetition rate and, if demanded, synchronized with a conventional high-intensity fs Ti:Sa laser. Unique experiments will become feasible with this machine on the non-linear interaction of high-energy light with ions, atoms, molecules, molecular ions, clusters and surfaces, only one of them being shortly sketched below.

We tune for example the VUV laser to an energy slightly above say the Ne K-shell binding energy  $E_{\text{bind}}$ . When hitting a Ne atom, a photoelectron will be emitted with an energy of  $E_e = h\nu - E_{\text{bind}}$  into the continuum which we assume to be modulated by a conventional fs laser at an intensity of  $1 \text{ PW/cm}^2$  as illustrated in Figure 7.

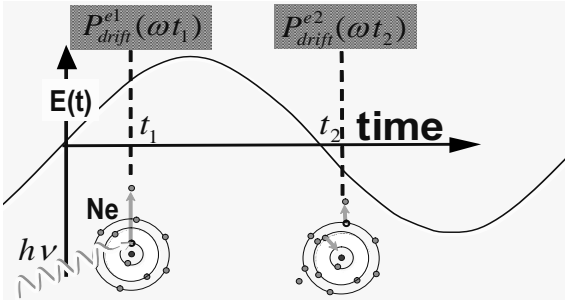


Figure 7: Illustration of the “attosecond streak camera”: At  $t_1$  a photoelectron is emitted due to inner-shell ionization by the FEL pulse. An optical laser pulse of  $1 \text{ PW/cm}^2$  at 800 nm, synchronized with the FEL, modifies the continuum.

Hence, the electron becomes an additional drift momentum proportional to the actual phase when it enters the continuum. If the linear polarization directions of both light fields are oriented perpendicular to each other, the modification of the continuum momentum by the optical laser is largely independent of the total electron energy which is determined by the VUV-light. Thus, the drift momentum and, therefore the phase of the field when the electron was emitted, can be measured with high accuracy (such a technique has recently been used to characterize an attosecond harmonic pulse [35]). After some time delay which is determined by the life-time of the innershell hole, a KLL Auger electron will be emitted, for example, with a characteristic energy that again is modified by the drift momentum in the external field. Measuring the correlated drift momenta of both electrons with an accuracy of 0.1 a.u. as routinely obtained in present laser experiments, will yield the time-correlation between both electrons with an estimated resolution of 80 as. In this scenario the “attosecond streak camera” only works in a unique way for time-delays of up to half an optical cycle which is about 1.3 fs for a Ti:Sa oscillator. This restriction, however, might be overcome if the polarization of the optical laser is time-dependently turned in such a way that the direction of the drift momenta give information about the number of optical cycles that have passed after the emission of the first electron. Still, the magnitude of the drift momentum will give the attosecond time resolution.

Many similar schemes might be envisaged to monitor the time-evolution of correlated atomic and molecular electronic processes on an attosecond time-scale. A factor of 10 better momentum resolution seems feasible, leading to a time-resolution of a few as. In order to succeed, large acceptance, high-resolution multi-electron spectrometers are indispensable as realized in our “reaction-microscopes”

## References

- [1] T. Brabec and F. Krausz, *Rev. Mod. Phys.* **72**, 545 (2000)
- [2] L. Di Mauro and P. Agostini, *Advances in Atomic and Molecular Physics* (Academic Press), New York (1995)
- [3] M. Protopapas, C. Keitel and P. Knight, *Physics Reports* **60**, 389 (1997)
- [4] P. Lambropoulos, P. Maragakis and J. Zhang, *Physics Reports* **305**, 203 (1998)
- [5] J. Ullrich et al., *J. Phys. B* **30**, 2917 (1997)
- [6] R. Dörner et al., *Physics Reports* **330**, 96 (2000)
- [7] R. Dörner et al., *Adv. in Atom., Mol., and Opt. Physics* **48** (2002) in print
- [8] R. Moshhammer et al., *Nucl. Instr. Meth. B* **108**, 425 (1996)
- [9] R. Moshhammer et al., *Optics Express* **8**, 358 (2001).
- [10] E. Eremina et al., *Phys. Rev. Lett.* (2002) submitted
- [11] T. Weber et al., *Phys. Rev. Lett.* **84**, 443 (2000)
- [12] B. Feuerstein et al., *Phys. Rev. Lett.* **87**, 043003 (2001)
- [13] T. Weber, et al., *J. Phys B* **33**, L127 (2000)
- [14] S. Larochelle, A. Talebpour and S.L. Chin, *J. Phys B* **31**, 1201 (1998).
- [15] L.V. Keldysh, *Zh. Eksp. Teor. Fiz.* **47**, 1945 (1964)
- [16] R. Moshhammer et al., *Phys. Rev. Lett.* **84**, 447 (2000)
- [17] D.N. Fittinghoff et al., *Phys. Rev. Lett.* **69**, 2642 (1992)
- [18] U. Eichmann et al., *Phys. Rev. Lett.* **84**, 3550 (2000)
- [19] B. Feuerstein, R. Moshhammer and J. Ullrich, *J. Phys B* **33**, L823 (2000)
- [20] M. Y. Kuchiev, *Sov. Phys.-JETP Lett.* **45**, 404 (1987)
- [21] P. Corkum, *Phys. Rev. Lett.* **71**, 1994 (1993)
- [22] D. Fittinghoff et al., *Phys. Rev. A* **49**, 2174 (1994)
- [23] P. Dietrich et al, *Phys. Rev. A* **50**, R3585 (1994)
- [24] B. Feuerstein et al., *Phys. Rev. Lett.* **87**, 043003 (2001)
- [25] T. Weber et al., *Nature* **404**, 608 (2000)
- [26] S. Goreslavskii and S. Popruzhenko, *Optics Express* **8**, 395 (2001).
- [27] J. Chen et al., *Phys. Rev.* **63**, 011404R (2000)
- [28] M. Lein, E. Gross and V. Engel, *Phys. Rev. Lett.* **85**, 4707 (2000)
- [29] R. Moshhammer et al., *Phys. Rev. A* **65**, 035401(2002)
- [30] M. Weckenbrock et al., *J. Phys. B* **34**, L449 (2001)
- [31] J. S. Parker et al., *J. Phys. B* **34**, L691 (2001)
- [32] H. Rottke et al., *Phys. Rev. Lett.* (2002) accepted
- [33] M. Drescher et al., *Science* **291**, 1923 (2001)
- [34] Th. Möller et al., *Phys. Rev. Lett.* (2002) submitted
- [35] M. Hentschel et al., *Nature* **413**, 509 (2001)